

# Gutmann Acceptor Properties of LiCl, NaCl, and KCl Buffered Ambient-Temperature Chloroaluminate Ionic Liquids

Robert A. Mantz, Paul C. Trulove,<sup>†</sup> Richard T. Carlin,<sup>‡</sup> Terry L. Theim,<sup>§</sup> and Robert A. Osteryoung\*

Department of Chemistry, North Carolina State University, Raleigh, North Carolina 27695-8204

Received August 14, 1996<sup>Ⓢ</sup>

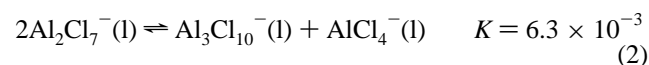
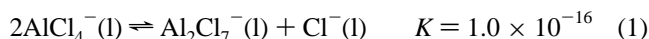
Gutmann acceptor numbers have been determined using <sup>31</sup>P nuclear magnetic resonance (NMR) for AlCl<sub>3</sub>/EMIC melts as well as LiCl, NaCl, and KCl neutral buffered melts. In AlCl<sub>3</sub>/EMIC melts, where EMIC is 1-ethyl-3-methylimidazolium chloride, the change in Gutmann acceptor number as a function of the AlCl<sub>3</sub>:EMIC melt ratio is attributed to an equilibrium between a monoadduct of triethylphosphine oxide·AlCl<sub>3</sub> and a diadduct of triethylphosphine oxide·2AlCl<sub>3</sub>. Observed acceptor numbers for the neutral buffered melts appear linear with respect to the melt's initial mole ratio of AlCl<sub>3</sub>:EMIC prior to buffering. The lithium cation appears to be the most Lewis acidic alkali metal cation followed by the sodium and potassium cations. Possible reasons for the change in acceptor number as a function of changing alkali metal cation concentration are presented.

## Introduction

Ambient-temperature chloroaluminate ionic liquids are an important class of nonaqueous solvents; they have been used for a wide variety of chemical and electrochemical studies.<sup>1–4</sup> In addition, they show promise as electroplating baths for industrial aluminum electroplating, as well as electrolytes in high-energy density batteries.<sup>5–7</sup>

The chloroaluminate ionic liquids we are studying are mixtures of 1-ethyl-3-methylimidazolium chloride (EMIC) and aluminum chloride (AlCl<sub>3</sub>). The two solids react over a wide range of stoichiometries to yield room-temperature molten salts.<sup>5</sup> The melts are defined as acidic, basic, or neutral if the mole ratio of AlCl<sub>3</sub> to EMIC is greater than, less than, or equal to unity. The chemistry of solutes observed in the melts is strongly affected by melt composition. This change in chemistry is due to the change in anionic speciation of the melt with composition.

Melt anionic composition is controlled by two equilibria, the first of which is analogous to the autoprotolysis of water.<sup>8</sup>



<sup>†</sup> Present address: Chemistry Department, U.S. Naval Academy, 572 Holloway Rd., Annapolis, MD 21402-5026.

<sup>‡</sup> Present address: Covalent Associates, Inc., 10 State St., Woburn, MA 01801.

<sup>§</sup> Present address: Chemistry Department, U.S. Air Force Academy, CO 80840.

<sup>Ⓢ</sup> Abstract published in *Advance ACS Abstracts*, February 1, 1997.

- (1) Gale, R. J.; Osteryoung, R. A. In *Molten Salt Techniques*; Lovering, D. G., Gale, R. J., Eds.; Plenum: New York, 1983; Vol. 1, pp 55–78.
- (2) Hussey, C. L. *Adv. Molten Salt Chem.* **1983**, *5*, 185–230.
- (3) Osteryoung, R. A. In *Molten Salt Techniques*; Mamantov, G., Marassi, R., Eds.; NATO ASI Series C, Vol. 202; Reidel: Dordrecht, The Netherlands, 1986; pp 329–64.
- (4) Hussey, C. L. *Pure Appl. Chem.* **1988**, *60*, 1763–72.
- (5) Wilkes, J. S.; Levisky, J. A.; Wilson, R. A.; Hussey, C. L. *Inorg. Chem.* **1982**, *21*, 1263–4.
- (6) Fannin, A. A., Jr.; Floreani, D. A.; King, L. A.; Sanders, J. S.; Piersma, B. J.; Stech, D. J.; Vaughn, R. L.; Wilkes, J. S.; Williams, J. L. *J. Phys. Chem.* **1984**, *88*, 2614.
- (7) Floreani, D.; Stech, D.; Wilkes, J.; Williams, J.; Piersma, B.; King, L.; Vaughn, R. In *Proceedings of the 30th Power Sources Symposium*; The Electrochemical Society: Pennington, NJ, 1982; p 84.

In basic melts, added aluminum chloride is neutralized by reaction with the chloride anion. As the mole ratio of the two components approaches 1.0:1.0, the Cl<sup>−</sup> concentration drops until the melt contains only the AlCl<sub>4</sub><sup>−</sup> anion. At mole ratios greater than 1.0:1.0, the Al<sub>2</sub>Cl<sub>7</sub><sup>−</sup> mole fraction increases and the AlCl<sub>4</sub><sup>−</sup> mole fraction decreases. However, if the mole ratio is increased to 1.6:1.0 or higher, the AlCl<sub>4</sub><sup>−</sup> mole fraction continues to drop and the Al<sub>2</sub>Cl<sub>7</sub><sup>−</sup> mole fraction peaks and then declines as the Al<sub>3</sub>Cl<sub>10</sub><sup>−</sup> mole fraction grows in.<sup>8</sup>

Neutral buffered chloroaluminate melts are prepared by the addition of an alkali metal chloride (MCl) to an acidic melt.<sup>8,9</sup> The reaction

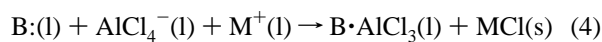


takes place when MCl is added to an acidic melt. The melt that results only contains the Lewis neutral anion, AlCl<sub>4</sub><sup>−</sup>, so it is no longer acidic. The electrochemical window of these neutral buffered melts is essentially the same as that of the neutral unbuffered melts.<sup>8</sup> Neutrality is maintained in neutral buffered melts regardless of the addition of strong Lewis acids or bases. If a strongly acidic species, such as aluminum chloride, is added to the melt, excess MCl dissolves and reacts to bring the melt back to neutrality. If a strongly basic species, such as chloride, is added to the melt, the dissolved M<sup>+</sup> reacts to form MCl, which is insoluble in a neutral melt and precipitates out of solution.

The neutral buffered melts have a property that we have termed “latent acidity”.<sup>10,11</sup> This is observed when certain weak Lewis bases (B:) are added to a neutral buffered melt. If the M<sup>+</sup> concentration exceeds the base concentration, then all of the base forms an AlCl<sub>3</sub> adduct. When the base concentration exceeds the M<sup>+</sup> concentration, the adduct is only formed up to the M<sup>+</sup> concentration; the excess base does not form an AlCl<sub>3</sub> adduct.<sup>11</sup> The formation of the adduct is driven by the reaction of M<sup>+</sup> with Cl<sup>−</sup>, which is liberated as the AlCl<sub>4</sub><sup>−</sup> ion forms an

- (8) Melton, T. J.; Joyce, J.; Maloy, J. T.; Boon, J. A.; Wilkes, J. S. *J. Electrochem. Soc.* **1990**, *137*, 3865–9.
- (9) Scordilis-Kelley, C.; Fuller, J.; Carlin, R. T.; Wilkes, J. S. *J. Electrochem. Soc.* **1992**, *139*, 694–9.
- (10) Quarmby, I. C.; Osteryoung, R. A. *J. Am. Chem. Soc.* **1994**, *116*, 2649–50.
- (11) Quarmby, I. C.; Mantz, R. A.; Osteryoung, R. A. *Anal. Chem.* **1994**, *66*, 3558–61.

$\text{AlCl}_3$  adduct with B:



The  $\text{AlCl}_3$  adduct formation has been attributed to the driving force provided by the precipitation of  $\text{MCl}$  from solution. When all of the metal cation has precipitated as the metal chloride, a driving force no longer exists; therefore no additional adduct is formed.

Gutmann acceptor numbers are a nonthermodynamic measure of the Lewis acidity of a solvent. They give a qualitative description of the solvent Lewis acidity and can be used to compare disparate solvents and to predict the chemistry of different solutes in these systems.<sup>12–14</sup> Prior work in this laboratory described the Gutmann donor and acceptor number parameters for 1-ethyl-3-methylimidazolium- and *N*-butylpyridinium-based chloroaluminate melts.<sup>15</sup> However, since that time “neutral buffered” chloroaluminate melts have emerged. These new ternary melts provide researchers with systems that allow additional control of the melt properties. The acidity of these new melts is of interest, and Gutmann acceptor numbers provide a way to make comparisons between the neutral buffered melts as well as between the neutral buffered melts and ethylmethylimidazolium-based melts.

The work reported here further characterizes these unique buffered chloroaluminate melt systems. A comparison is made between the Gutmann acceptor numbers of the  $\text{LiCl}$ ,  $\text{NaCl}$ , and  $\text{KCl}$  neutral buffered melts and the binary  $\text{AlCl}_3/\text{EMIC}$  melts, and the variation in acceptor number with melt composition is discussed for the four systems.

## Experimental Section

The preparation of EMIC has been described previously.<sup>5,16</sup>  $\text{AlCl}_3$  was of Fluka purissimo grade and was purified as described elsewhere.<sup>1</sup> All melt preparations and handling were carried out in a helium-filled Vacuum Atmospheres drybox with oxygen and water levels less than 5 ppm. Melts were prepared by combining weighed portions of  $\text{AlCl}_3$  with EMIC in Qorpak bottles to yield a slightly basic melt (0.99:1.00). The melts were filtered with 1  $\mu\text{m}$  glass Acrodisk filters. Proton impurities were removed using vacuum ( $4 \times 10^{-5}$  Torr).<sup>17</sup> Oxide was removed by exposing the melt to phosgene twice, and protons were again removed under vacuum.<sup>18</sup> A weighed amount of  $\text{AlCl}_3$  was then added to a portion of the basic melt to yield the desired composition.  $\text{LiCl}$  (Aldrich, 99.994%),  $\text{NaCl}$  (Aldrich, 99.999%), and  $\text{KCl}$  (Aldrich, 99.999%) were dried at 400 °C under vacuum ( $1 \times 10^{-3}$  Torr) for at least 3 days. The weight percent of metal chloride required to buffer a melt was determined from the  $\text{Al}_2\text{Cl}_7^-$  concentration in the unbuffered melt. Buffered melts were prepared by the addition of 150 wt % of the metal chloride required to neutralize the acidic melt. The melt was then allowed to stir for at least 24 h while being warmed on a stirrer hot plate ( $\approx 60$  °C). Triethylphosphine oxide (TEPO) (Alfa) was purified by sublimation under vacuum ( $1 \times 10^{-3}$  Torr) at room temperature and collected in a trap held at 0 °C prior to use.<sup>13</sup> Nuclear magnetic resonance (NMR) tubes were prepared by soaking in 50%  $\text{HNO}_3$  heated to 90 °C, rinsing with deionized water, soaking in a solution of the tetrasodium salt of EDTA for 12 h at room temperature, and again rinsing with deionized water.  $^{31}\text{P}$  NMR spectra were obtained

with a Bruker AC-300 NMR spectrometer operating at 121.50 MHz. The probe temperature was maintained at 31.0 °C, and each sample was allowed to equilibrate while rotating at 10 Hz for at least 5 min prior to spectral acquisition. Spectra consisted of 64 scans with a sweep width of 128.6 ppm and a relaxation delay time of 2.0 s. An exponential multiplication with a line broadening of 2.0 Hz was applied to the acquired free induction decay (FID). The chemical shift was externally referenced to an 85% phosphoric acid in water sample (0 ppm) whose spectrum was obtained using identical acquisition and processing parameters.

Experiments were conducted to determine the change in chemical shift of the triethylphosphine oxide (TEPO) versus the concentration of the TEPO in the melt. Four melts were prepared, a 1.30:1.00 melt, a 1.15:1.00  $\text{LiCl}$  buffered melt, a 1.30:1.00  $\text{NaCl}$  buffered melt, and a 1.30:1.00  $\text{KCl}$  buffered melt. Each melt was divided into six portions, and TEPO was added to make 5, 10, 25, 50, 100, and 300 mM solutions. The solutions were allowed to stir for 24 h at  $\approx 60$  °C to ensure complete dissolution of the TEPO. After being stirred for 24 h, the samples were allowed to cool to room temperature. The resultant solution was filtered through a 0.1  $\mu\text{m}$  PTFE (Whatman) filter disk (13 mm diameter) using a 5 mL syringe (B&D tuberculin, polyethylene, natural rubber latex) into a 9 in. long 10 mm Wilmad NMR tube that had been constricted at 8 in. For the buffered melts a tip-off manifold was placed on each tube, and the sealed assembly was removed from the drybox and flame-sealed under vacuum ( $\approx 1 \times 10^{-2}$  Torr). The unbuffered melts were capped and sealed with Parafilm.  $^{31}\text{P}$  NMR spectra were obtained for each sample.

Experiments were conducted to determine the change in the chemical shift of the TEPO versus the melt composition. Melt compositions of the unbuffered and of  $\text{LiCl}$ ,  $\text{NaCl}$ , and  $\text{KCl}$  buffered melts corresponded to initial  $\text{AlCl}_3/\text{EMIC}$  mole ratios of 1.05:1.00, 1.10:1.00, 1.15:1.00, 1.20:1.00, 1.30:1.00, 1.40:1.00, 1.50:1.00, 1.70:1.00, and 1.90:1.00. In addition, an unbuffered melt with a mole ratio of 0.99:1.00 was prepared. TEPO was added to each melt to make 10 mM solutions. The solutions were prepared as described above.  $^{31}\text{P}$  NMR spectra were obtained for each sample.

To determine what causes the small downfield peak observed in some of the  $^{31}\text{P}$  NMR spectra, three samples whose preparation is described above were modified. These three samples consisted of a 1.30:1.00 unbuffered melt containing 50, 100, and 300 mM TEPO. To the 100 and 300 mM TEPO-containing melts was added 1-ethyl-3-methylimidazolium hydrogen dichloride so that the same concentrations of  $\text{HCl}$  and TEPO were present in the melt.<sup>19</sup> A 10-fold excess of  $\text{H}_2\text{O}$  was added to the sample containing 50 mM TEPO. This sample was warmed and stirred for several hours to allow the water to fully react and to allow the resulting crust to dissolve in the melt. The samples were flame-sealed under vacuum as described above.

Volume magnetic susceptibilities were determined using a variation of Becconsall's method.<sup>20,21</sup> Samples were prepared by flame sealing benzene- $d_6$  in the inner coaxial tube from a Wilmad 10 mm coaxial tube pair. The melt of interest was placed in the outer tube to which approximately 5% by weight of benzene- $d_6$  had been added. The chemical shift of the benzene- $d_6$  dopant in the outer tube did not appear to change due to any reaction between the melt and the benzene, although the benzene does decompose over time. The inner coaxial tube was inserted into the 10 mm NMR tube, and the entire apparatus was then capped and sealed with Parafilm. These samples were analyzed in both a Bruker AC-300 (75.47 MHz) and a JEOL FX-90Q (22.48 MHz) using  $^{13}\text{C}$  NMR. The probe on each spectrometer was maintained at 31 °C, and each sample was allowed to equilibrate for at least 5 min while being rotated at 10 Hz in the Bruker and 15–20 Hz in the JEOL prior to spectral acquisition. Each spectrometer was locked on the benzene- $d_6$  in the sample. Spectra obtained on the Bruker AC-300 consisted of 16 scans with a sweep width of 161.6 ppm and a relaxation delay time of 2.0 s. An exponential multiplication with a line broadening of 2.0 Hz was applied to the acquired FID. Spectra

(12) Gutmann, V. *The Donor-Acceptor Approach to Molecular Interactions*; Plenum Press: New York, 1978.

(13) Mayer, U.; Gutmann, V.; Gerger, W. *Monatsh. Chem.* **1975**, *106*, 1235–57.

(14) Gutmann, V. *Electrochim. Acta* **1976**, *21*, 662–70.

(15) Zawodzinski, T. A., Jr.; Osteryoung, R. A. *Inorg. Chem.* **1989**, *28*, 1710–5.

(16) Trulove, P. C.; Osteryoung, R. A. *Inorg. Chem.* **1992**, *31*, 3980–5.

(17) Noël, M. A.; Trulove, P. C.; Osteryoung, R. A. *Anal. Chem.* **1991**, *63*, 2892–6.

(18) Sun, I. W.; Ward, E. H.; Hussey, C. L. *Inorg. Chem.* **1987**, *26*, 4309–11.

(19) Zawodzinski, T. A., Jr.; Osteryoung, R. A. *Inorg. Chem.* **1988**, *27*, 4383–4.

(20) Becconsall, J. K.; Daves, G. D., Jr.; Anderson, W. R., Jr. *J. Am. Chem. Soc.* **1970**, *92*, 430–2.

(21) Becker, E. D. *High Resolution NMR: Theory and Chemical Applications*, 2nd ed.; Academic Press: New York, 1980; pp 59–61.

acquired on the JEOL FX-90Q consisted of 64 scans with a sweep width of 111.0 ppm and a relaxation delay of 2.0 s. An exponential multiplication with a line broadening of 1.0 Hz was applied to the acquired FID. The volume magnetic susceptibility was then calculated from the differences in  $^{13}\text{C}$  chemical shifts with the two different field axes between the benzene- $d_6$  in the inner and annular regions of the coaxial pair.

Assuming cylindrical samples of infinite length, the chemical shift contribution due to the volume bulk susceptibility for an electromagnet when the sample direction is perpendicular to the magnetic field is<sup>20</sup>

$$\delta_b^\perp = \frac{2}{3}\pi\chi_v \quad (5)$$

$\chi_v$  is the volume bulk magnetic susceptibility, and  $\delta_b$  is the bulk magnetic susceptibility contribution. With the sample assumptions stated above for a superconducting magnet, when the sample direction is parallel to the magnetic field, the chemical shift due to the volume bulk susceptibility is<sup>20</sup>

$$\delta_b^\parallel = -\frac{4}{3}\pi\chi_v \quad (6)$$

By comparing the same solvent in the inner and annular portions of a coaxial NMR tube and observing the chemical shift difference, one can solve for the volume magnetic susceptibility using the following two equations:<sup>20</sup>

$$\delta_{\text{sol}}^\perp(y) - \delta_{\text{sol}}^\perp(x) = \frac{2}{3}\pi[\chi_v(y) - \chi_v(x)] + \delta_{\text{loc}}(y) - \delta_{\text{loc}}(x) \quad (7)$$

$$\delta_{\text{sol}}^\parallel(y) - \delta_{\text{sol}}^\parallel(x) = -\frac{4}{3}\pi[\chi_v(y) - \chi_v(x)] + \delta_{\text{loc}}(y) - \delta_{\text{loc}}(x) \quad (8)$$

$\delta_{\text{sol}}$  in these two equations is the observed difference in chemical shift.  $\delta_{\text{loc}}$  is the chemical shift difference due to "local" effects (effects other than bulk susceptibility).  $y$  is the solvent whose magnetic susceptibility is being determined, and  $x$  is a solvent with known magnetic susceptibility.  $\delta_{\text{loc}}$  is what is actually measured experimentally. Combining the above equations results in<sup>20</sup>

$$\delta_{\text{loc}}(y) - \delta_{\text{loc}}(x) = \frac{1}{3}[\delta_{\text{sol}}^\parallel(y) - \delta_{\text{sol}}^\parallel(x) + 2(\delta_{\text{sol}}^\perp(y) - \delta_{\text{sol}}^\perp(x))] \quad (9)$$

$\delta_{\text{sol}}$  is the measured chemical shift of the solvent in the coaxial NMR tube. After measurement of the chemical shift differences in both the electromagnet and the superconducting magnet,  $\delta_{\text{loc}}(y) - \delta_{\text{loc}}(x)$  can be calculated. Next, this value is substituted into either eq 5 or eq 6 to give

$$\chi_v^\perp = \frac{3}{2\pi}(\delta_{\text{loc}}^\perp(y) - \delta_{\text{loc}}^\perp(x)) \quad (10)$$

$$\chi_v^\parallel = -\frac{3}{4\pi}(\delta_{\text{loc}}^\parallel(y) - \delta_{\text{loc}}^\parallel(x)) \quad (11)$$

$\chi_v^\perp$  should equal  $\chi_v^\parallel$ . Finally, this  $\chi_v$  must be corrected using the  $x$  solvent magnetic susceptibility, which is known.

$$\chi_v(y) = \chi_v(x) + \chi_v^\parallel \quad (12)$$

Once the magnetic susceptibility is known, the correction to the chemical shift in a superconducting magnet is calculated using

$$\delta_{\text{cor}} = -\frac{4}{3}\pi(\chi_v(\text{hexane}) - \chi_v(\text{melt})) \quad (13)$$

Neutral buffered melt samples for inductively coupled plasma (ICP) analyses were prepared by first pipetting 100  $\mu\text{L}$  of melt into a 100 mL volumetric flask. The flask was then fitted with a rubber septum and removed from the drybox. Approximately 20 mL of water (18 M $\Omega$ ) was added through the septum with a syringe and needle. The water was then swirled until all the melt dissolved. Finally, the septum was removed and water added till the volume totaled 100 mL.

Elemental analyses were performed by using a Leeman PS Series 1000 sequential ICP (Leeman Labs, Lowell, MA) with an Echelle spectrometer and Hildebrand Grid nebulizer system. The ICP is a computer-controlled, sequential instrument allowing rapid elemental

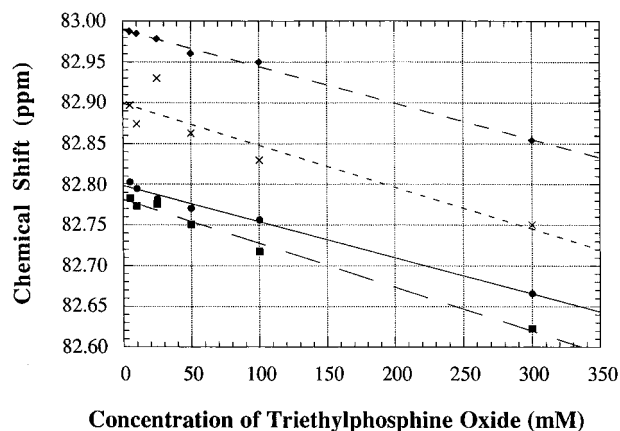


**Figure 1.**  $^{31}\text{P}$  NMR chemical shift dependence of triethylphosphine oxide upon the concentration of triethylphosphine oxide in the melt: ●, acidic melt; ■, LiCl buffered melt; ◆, NaCl buffered melt; ×, KCl buffered melt.

**Table 1.**  $^{31}\text{P}$  NMR Chemical Shift Dependence on TEPO Concentration

$$^{31}\text{P NMR shift (ppm)} = m[\text{TEPO (mM)}] + b$$

melt	$m$	$b$
unbuffered	$-4.4 \times 10^{-4} \pm 2 \times 10^{-5}$	$82.798 \pm 0.003$
LiCl buffered	$-5.3 \times 10^{-4} \pm 3 \times 10^{-5}$	$82.781 \pm 0.003$
NaCl buffered	$-4.4 \times 10^{-4} \pm 2 \times 10^{-5}$	$82.989 \pm 0.002$
KCl buffered	$-5 \times 10^{-4} \pm 1 \times 10^{-4}$	$82.90 \pm 0.01$

analysis. Each element was determined using the emission lines 670.784 nm for lithium, 589.592 nm for sodium, and 766.490 nm for potassium. Additional instrumental parameters used for this study were 1.0 kW of power, a 40.68 MHz Flagg oscillator, a 14 L/min coolant flow rate, a nebulizer pressure of 40 psi, and a sample introduction of 1.0 mL/min.

**Safety Note.** Phosgene is an extremely toxic gas which should be used with caution.<sup>22</sup> A phosgene detector, Matheson Model 8014LA, toxic gas detector, was used to test for leaks in the apparatus employed. In addition, the phosgene procedure was conducted in a well-ventilated laboratory hood.<sup>17</sup>

## Results and Discussion

$^{31}\text{P}$  NMR spectra of pure solutions of triethylphosphine oxide (TEPO) in all melts generally consisted of a single line and did not change over the course of several days. The  $^{31}\text{P}$  NMR chemical shift data must be corrected prior to acceptor number determination. The first correction is the extrapolation of the  $^{31}\text{P}$  chemical shift to infinite dilution of TEPO in the melt. The second correction is for the contribution made to the observed  $^{31}\text{P}$  chemical shift by the volume bulk magnetic susceptibility ( $\chi_v$ ).

The effect of the TEPO concentration on the  $^{31}\text{P}$  chemical shift was determined for  $\text{AlCl}_3/\text{EMIC}$  melts as well as melts buffered with lithium, sodium, and potassium chloride. A linear equation was fitted to the resultant data and the resultant function extrapolated to infinite dilution (Figure 1 and Table 1). The TEPO concentration used to determine the acceptor numbers was 10 mM, thus the correction by extrapolating to infinite dilution of TEPO was  $\approx 0.005$  ppm.

Correction for magnetic susceptibility effects required additional experiments as mentioned above but did result in a much larger chemical shift correction, approximately 1 ppm. The magnetic susceptibility was measured as outlined previously, and a linear function was fit to the data (Figure 2 and Table 2).

(22) *The Merck Index*, 11th ed.; Budavari, S., O'Neil, M. J., Smith, A., Heckelman, P. E., Eds.; Merck & Co.: Rahway, NJ, 1989; p 1165.

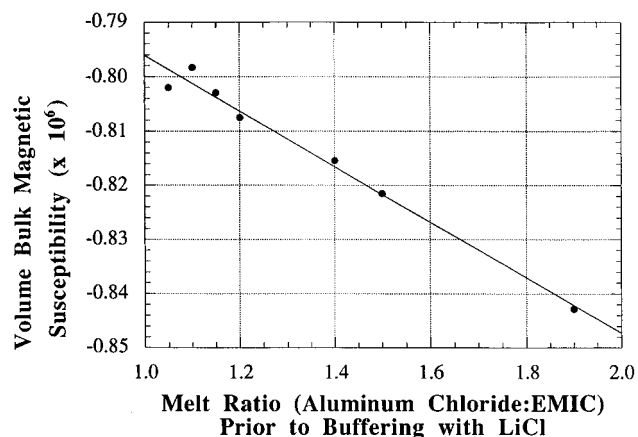


**Figure 2.** Volume bulk magnetic susceptibility of LiCl neutral buffered  $\text{AlCl}_3/\text{EMIC}$  ionic liquid.

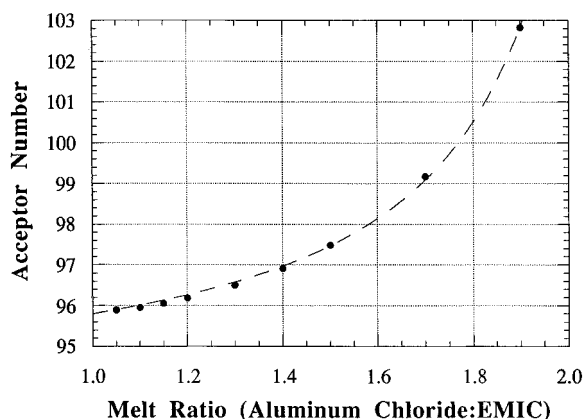


**Figure 3.** Dependence of the Gutmann acceptor number for binary melts upon the mole ratio of  $\text{AlCl}_3$  to EMIC. Points are experimental data, while the line is the fit using eq 17.

**Table 2.** Volume Bulk Magnetic Susceptibility of Melts

$$\text{magnetic susceptibility } (\times 10^6) = m(\text{melt ratio}) + b$$

melt	<i>m</i>	<i>b</i>
unbuffered	$-0.034 \pm 0.003$	$-0.759 \pm 0.004$
LiCl buffered	$-0.051 \pm 0.003$	$-0.745 \pm 0.004$
NaCl buffered	$-0.031 \pm 0.006$	$-0.769 \pm 0.008$
KCl buffered	$-0.09 \pm 0.06$	$-0.69 \pm 0.06$

This resultant function was then used to determine the chemical shift correction necessary for each melt composition.

Experiments were conducted in which the melt composition and the buffering alkali metal chloride were varied. After application of both corrections to the observed chemical shift data, the data were converted into Gutmann acceptor numbers using<sup>12</sup>

$$\text{AN} = 2.348\delta_{\text{cor}} \quad (14)$$

$\delta_{\text{cor}}$  is the  $^{31}\text{P}$  chemical shift using TEPO in hexane as the zero reference chemical shift (Figures 3 and 4). It should be noted that the melt ratio in the neutral buffered cases is the original melt ratio prior to addition of alkali halide. After buffering, the only anion present is  $\text{AlCl}_4^-$  and the alkali metal concentration is equal to the original  $\text{Al}_2\text{Cl}_7^-$  concentration.

In addition, a series of experiments were conducted in which ICP was used to determine the lithium, sodium, and potassium concentrations in the different compositions of neutral buffered melts (Figure 5). These data were originally obtained with units of parts per million. In order to allow direct comparison between the different alkali metals, these data were corrected

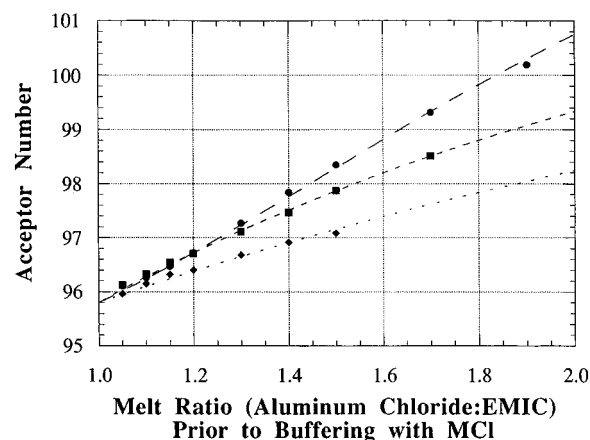


**Figure 4.** Dependence of the Gutmann acceptor number for alkali metal chloride neutral buffered melts upon the mole ratio of  $\text{AlCl}_3$  to EMIC. (Note: This is the mole ratio prior to buffering. During buffering, the  $\text{Al}_2\text{Cl}_7^-$  anions react with an equal number of alkali metal chlorides.) The data fit was performed using the equilibrium expression from the text: ●, LiCl buffered melt; ■, NaCl buffered melt; ◆, KCl buffered melt.

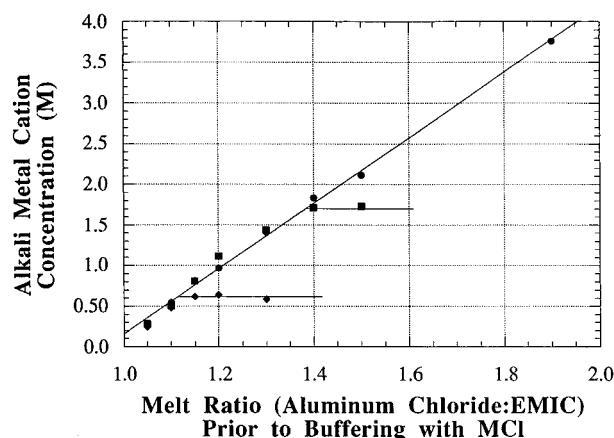


**Figure 5.** Alkali metal cation concentration determined using ICP versus mole ratio of  $\text{AlCl}_3$  to EMIC prior to buffering: ●, LiCl buffered melt; ■, NaCl buffered melt; ◆, KCl buffered melt.

by dividing each data point by the atomic weight of the alkali metal. One experimental complication was revealed by the ICP data, which were obtained much later than the NMR data. The ICP data for both the NaCl and KCl neutral buffered melts show a plateau for the alkali metal concentration at lower mole ratios even though the NMR data showed Gutmann acceptor number changes in the same region. This indicates that the NaCl and KCl neutral buffered melts prepared from acidic melts with mole ratios greater than  $\approx 1.1:1.0$  for KCl and  $\approx 1.4:1.0$  for NaCl were initially supersaturated.

More importantly, the ICP results represent the first determination of the extent of buffering possible with different alkali metal chloride salts. When an acidic melt is buffered with an alkali metal chloride salt, usually the metal salt dissolves as it reacts with the  $\text{Al}_2\text{Cl}_7^-$  and excess metal chloride salt remains in solid form. In some cases, when the melt was heated, the alkali metal salt would dissolve, but upon cooling a solid would precipitate. In these cases we found that as we increased the initial concentration of  $\text{Al}_2\text{Cl}_7^-$ , more solid would precipitate. This solid is presumably  $\text{MAlCl}_4$ . The buffering limit would therefore depend upon the solubility of  $\text{MAlCl}_4$  in a neutral melt. When the solubility limit has been reached,  $\text{MAlCl}_4$  will precipitate from solution. If a melt contains additional  $\text{Al}_2\text{Cl}_7^-$ , the MCl will continue to react with the additional  $\text{Al}_2\text{Cl}_7^-$  as the  $\text{MAlCl}_4$  that is formed precipitates. Therefore, the solu-

**Table 3.** Gutmann Acceptor Numbers of Alkali Metal Chloride Neutral Buffered Melts
$$AN = m(\text{melt ratio}) + b$$

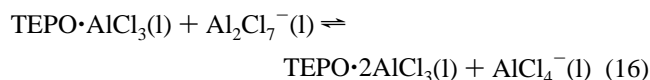
buffering agent	<i>m</i>	<i>b</i>	<i>R</i> <sup>2</sup>
LiCl	4.97 ± 0.08	90.8 ± 0.1	0.9981
NaCl	3.70 ± 0.06	92.28 ± 0.08	0.9982
KCl	2.5 ± 0.1	93.4 ± 0.1	0.9888

bility limit of MAICl<sub>4</sub> defines the maximum concentration of metal cation in solution. Using ICP, the solubility of MAICl<sub>4</sub> was determined, and the buffering limits were determined for LiCl, NaCl, and KCl neutral buffered melts. The buffering ability of LiCl is greater than an initial mole ratio of 1.9:1.0, whereas for NaCl the limit is ≈1.4:1.0 and for the KCl it is ≈1.1:1.0.

The results for the binary AlCl<sub>3</sub>/EMIC melts have been interpreted on the basis of earlier results, which demonstrated that the observed acceptor number in binary AlCl<sub>3</sub>/EMIC was a function of melt composition.<sup>15</sup> Our results for the binary melts are in agreement with this prior work. In basic and neutral melts, the acceptor number is a constant 95.8 for an AlCl<sub>3</sub> monoadduct and does not change. This appears to be due to solvent leveling (eq 15).<sup>15</sup> In melts with acidic compositions,



the change in acceptor number is due to the formation of a TEPO·2AlCl<sub>3</sub> diadduct caused by the strong Lewis acidity of Al<sub>2</sub>Cl<sub>7</sub><sup>-</sup> (eq 16). Only a single <sup>31</sup>P NMR peak is observed,



indicating the monoadduct and diadduct species are in fast equilibrium on the NMR time scale. Thus, contributions from both sides of the equilibrium (eq 16) must be considered. The observed chemical shift is a weighted average of the concentration of the two species multiplied by their respective chemical shifts. The acceptor number is directly related to the <sup>31</sup>P NMR chemical shift (eq 14). In order to quantitate this observed phenomenon, the equilibrium constant based on the above equation and the anionic composition were calculated for each melt composition. Because significant contributions from Al<sub>3</sub>Cl<sub>10</sub><sup>-</sup> are present only in melt compositions above ≈1.7:1.0 (AlCl<sub>3</sub>:EMIC), melt compositions were calculated by neglecting the Al<sub>3</sub>Cl<sub>10</sub><sup>-</sup> contributions and considering only AlCl<sub>4</sub><sup>-</sup> and Al<sub>2</sub>Cl<sub>7</sub><sup>-</sup> contributions. Fitting the results with eq 16 gives an equilibrium constant *K* for eqs 16 and 17 of 0.158 ± 0.008, an

$$AN = \frac{95.8}{\frac{\text{equil const} \times [\text{Al}_2\text{Cl}_7^-]}{[\text{AlCl}_4^-]} + 1} + \frac{\text{diadduct AN}}{\frac{[\text{Al}_2\text{Cl}_7^-]}{\text{equil const} \times [\text{AlCl}_4^-]} + 1} \quad (17)$$

acceptor number for the diadduct of 108.1 ± 0.3, and *R*<sup>2</sup> of 0.9993 (Figure 3). Employing a function that contains the Al<sub>3</sub>Cl<sub>10</sub><sup>-</sup> contributions simply results in greater uncertainty for the equilibrium constants and the diadduct acceptor number. It should be noted that, given the data above, the maximum acceptor number that is theoretically possible is ≈108, and it should also be noted that the magnitude of *K* shows that, even

at large Al<sub>2</sub>Cl<sub>7</sub><sup>-</sup> concentrations, there is only a small amount of diadduct formed. The TEPO·AlCl<sub>3</sub> monoadduct is such a weak base that Al<sub>2</sub>Cl<sub>7</sub><sup>-</sup> does not react with it to any substantial degree.

To calculate the Gutmann acceptor number (AN) of a binary melt of known composition, the AlCl<sub>4</sub><sup>-</sup> and Al<sub>2</sub>Cl<sub>7</sub><sup>-</sup> anionic mole fractions must first be calculated from the melt ratio.<sup>8</sup> Substituting these values into eq 18 gives the expected Gutmann

acceptor number for the melt:

$$AN = \frac{95.8}{\frac{0.158[\text{Al}_2\text{Cl}_7^-]}{[\text{AlCl}_4^-]} + 1} + \frac{108.1}{\frac{[\text{AlCl}_4^-]}{0.158[\text{Al}_2\text{Cl}_7^-]} + 1} \quad (18)$$

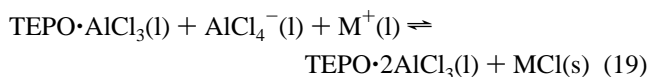
The determination of the acceptor numbers of the alkali metal neutral buffered melts was completed in the same fashion as those for the binary melts using eq 14. The plot of acceptor number versus AlCl<sub>3</sub>:EMIC melt ratio prior to buffering is linear. It is important to remember that the melt ratio prior to buffering corresponds to the alkali metal cation concentration in the buffered melt. The linear function results in very good fits for the LiCl, NaCl, and KCl buffered melts, *R*<sup>2</sup> equals 0.9981, 0.9982, and 0.9888, respectively (Figure 4 and Table 3). Using the linear functions for each of the three types of buffered melts, the acceptor numbers can be predicted. It should be noted that because the melts prior to buffering are acidic and because the neutral buffered melts still appear more acidic than the basic melts, no anionic species such as LiCl<sub>2</sub><sup>-</sup>, which has been observed in basic melts, are expected to be present.

Attempts to model the neutral buffered melts are not nearly so straightforward as those for the binary melts. The results for the neutral buffered melts can be interpreted in two ways. Both models explain portions of the data better, but neither offers an all-encompassing explanation for the observed data.

In the first model, the observed acceptor number is simply a function of two different ionic systems, EM<sup>+</sup>/AlCl<sub>4</sub><sup>-</sup> and M<sup>+</sup>/AlCl<sub>4</sub><sup>-</sup>. In the second model, the observed acceptor number is a function of an equilibrium between a TEPO·AlCl<sub>3</sub> monoadduct and a TEPO·2AlCl<sub>3</sub> diadduct formed via the driving force provided by the precipitation of the an alkali metal chloride salt.

On the basis of the first model, one would expect the observed acceptor number to simply be a weighted average of the acceptor numbers of the two types of melt based upon the mole fractions. When the data are plotted in this fashion, the lines are curvilinear for each of the melts (Figure 6). This can be attributed to preferential solvation by one of the components of the melts.<sup>12</sup> The differences between alkali metal chloride neutral melts buffered with different alkali metal chlorides appear to correlate with the alkali metal cation size. The Li<sup>+</sup> cation, being the smallest cation, would be expected to approach the TEPO·AlCl<sub>3</sub> monoadduct more closely. A possible explanation for the nonlinearity is that the Li<sup>+</sup> cation is also the hardest and strongest Lewis acid of the three alkali metal cations. Because the TEPO·AlCl<sub>3</sub> monoadduct is a Lewis base, the Li<sup>+</sup> cation may preferentially solvate the TEPO·AlCl<sub>3</sub> monoadduct. The Na<sup>+</sup> cation would be expected to show less of this behavior and K<sup>+</sup> still less. Although the data seem to be in accord with these explanations, these observations are not quantifiable.

The second explanation uses a model similar to that for the binary melts and results in an equilibrium expression:



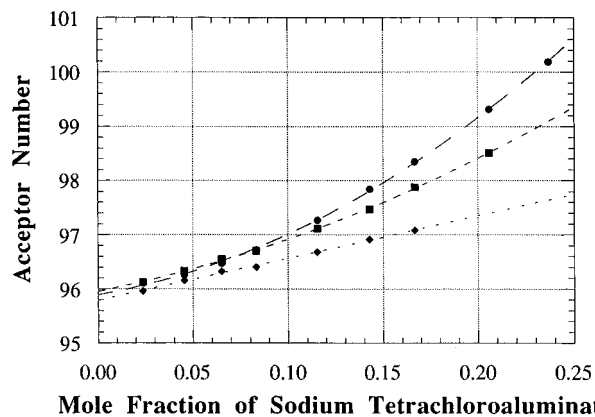


**Figure 6.** Dependence of the Gutmann acceptor number upon the mole fraction of alkali metal tetrachloroaluminate present in the ionic liquid: ●, LiCl buffered melt; ■, NaCl buffered melt; ◆, KCl buffered melt.

The driving force for this equilibrium is the precipitation of the alkali metal chloride. Using this model, the maximum acceptor number would be 108.1 as determined in the  $\text{AlCl}_3/\text{EMIC}$  melts. Using eq 19 to fit the data and using the diadduct acceptor number of 108.1 result in equilibrium constants  $K$  ( $\text{M}^{-2}$ ) of  $0.342 \pm 0.004$ ,  $0.27 \pm 0.01$ , and  $0.18 \pm 0.01$  for the lithium, sodium, and potassium buffered melts, respectively.  $R^2$  for each of the fits are 0.9980, 0.9540, and 0.9164, respectively. The magnitudes of the equilibrium constants are still relatively small. These results show quantitatively the differences between melts buffered with different alkali metal cations as well as the dependence of the acceptor number on the original melt composition prior to buffering. These results also fit the model presented by Zawodzinski et al.,<sup>15</sup> where the TEPO forms an aluminum chloride diadduct. It should also be noted that, because the equilibrium constants are small and because the melt ratios investigated only vary between 1.0:1.0 and 1.9:1.0, the expressions would be expected to appear linear.

These results indicate that the alkali metal buffered melts are more Lewis acidic than the  $\text{AlCl}_3/\text{EMIC}$  melts at low melt ratios (below mole ratios of  $\approx 1.4:1.0$ ). This was not expected and may only be true with the triethylphosphine oxide probe molecule. In addition, the  $R^2$  values for the data fit using eq 19 are not compelling.

For some samples, a very small downfield peak (larger chemical shift) in the  $^{31}\text{P}$  NMR spectrum appeared. Several experiments were conducted to determine the origin of this peak.

Protons in the form of 1-ethyl-3-methylimidazolium hydrogen dichloride were added to several samples.<sup>19</sup> To another sample was added water. Water acts not only as a proton source but also as an oxide source.<sup>23,24</sup> The sample to which the water had been added showed a marked increase in the intensity of the downfield peak. This suggests that the presence of the peak is due to either an aluminum oxide or an aluminum hydroxide species and that this species is more Lewis acidic than the native melt. The Lewis acidity of the oxide species has not been investigated to date, and further experiments are underway to investigate this phenomenon.

## Conclusions

Gutmann acceptor numbers of the  $\text{AlCl}_3/\text{EMIC}$  melts, as well as their alkali metal neutral buffered counterparts, have been determined. The data from the binary  $\text{AlCl}_3/\text{EMIC}$  melts have been fitted using the equilibrium expression derived from the model in which triethylphosphine oxide forms an  $\text{AlCl}_3$  diadduct with an acceptor number of 108.1. This expression allows us to predict the Gutmann acceptor number of binary  $\text{AlCl}_3/\text{EMIC}$  melts.

The Gutmann acceptor numbers of the alkali metal chloride neutral buffered melts can be predicted using a linear expression. The LiCl neutral buffered melts show the greatest Lewis acidity followed by the NaCl and the KCl buffered melts. These data indicate that the potassium chloride neutral buffered melt is more Lewis acidic than its binary counterpart up to an  $\text{AlCl}_3:\text{EMIC}$  mole ratio of 1.3:1.0; for the sodium chloride neutral buffered melt, this ratio is 1.6:1.0, while for the lithium chloride, it is 1.7:1.0. These results provide insight into the differences between the unbuffered and alkali metal buffered melts as well as between the different alkali buffered melts themselves.

The buffering capacities for the LiCl, NaCl, and KCl neutral buffered melts have been determined using ICP. The buffering limit for LiCl is greater than an  $\text{AlCl}_3:\text{EMIC}$  initial mole ratio of 1.9:1.0. The buffering limit for a NaCl buffered melt is  $\approx 1.4:1.0$ , and the buffering limit for a KCl buffered melt is  $\approx 1.1:1.0$ .

**Acknowledgment.** This work was supported in part by the Air Force Office of Scientific Research.

IC960994N

(23) Zawodzinski, T. A., Jr.; Osteryoung, R. A. *Inorg. Chem.* **1987**, *26*, 2920–2.

(24) Zawodzinski, T. A., Jr.; Osteryoung, R. A. *Inorg. Chem.* **1990**, *29*, 2842–7.